

# **Analyses of Non-premixed Flameholding Behind a Step in Supersonic Flow**

*Amit Thakur and Corin Segal  
Mechanical & Aerospace Engineering  
University of Florida, Gainesville FL 32611 USA*

## **Abstract**

Flameholding in supersonic flow depends on the local conditions in the recirculation region and the mass transfer into and out of this region. Large gradients in local gas composition and temperature exist in the recirculation region. Hence stability parameter correlations developed for premixed flames cannot be used to determine the blowout stability limits for non-premixed flames encountered in practical devices. In the present investigation, a rearward-facing step was used as a generic flameholder for non-premixed, supersonic flow. For non-reacting flow conditions, the fuel related parameters such as fuel type and injection pressure were varied. The local distribution of fuel mole fraction in the recirculation region and the shear layer formed behind the step was determined using acetone PLIF. These measurements were compared with fuel mole fraction measurements at selected locations in the recirculation region using a mass spectrometer. The experimental data will contribute to formulation of a stability parameter for non-premixed flames.

## **Introduction**

Flameholding requires the fluid residence time larger than the fuel reaction time, i.e., a suitably selected Damköhler number,  $Da = \tau_{\text{residence}} / \tau_{\text{reaction}} > 1$ . The flow has a short residence time in the supersonic combustion chamber and is of the order of only a few milliseconds. The chemical reaction times are similar to the flow residence time for hydrogen while the reaction times for hydrocarbons are much higher. A recirculation region that extends the residence time is therefore used. This flameholding region serves as a reservoir of hot pool of radicals that sustains the flame in the scramjet combustor and as a supplier of radicals helping to propagate combustion in the main supersonic flow.

A simple geometry to generate a flameholding region in supersonic flow is a rearward-facing step that generates a primary recirculation region in which mixing and combustion find the necessary residence time. The approaching airflow boundary layer separates at the step and forms a shear layer between the supersonic flow and the subsonic recirculation region. Depending on the amount of heat released in this region an expansion or a compression will dictate the length of the recirculation region. If fuel is injected into the recirculation region, shear layers appear around the jet boundaries in which the flame is initiated followed by mixing and heat exchange between the hot gases in the region. Thus a primary recirculation of gases exists that engulfs the recirculation region with additional smaller recirculations present. Even in a two-dimensional geometry, a complex 3-D flow pattern emerges. In this region, large local equivalence ratio can exist even when the global equivalence ratio indicates an overall lean mixture<sup>1</sup>. The air mass flow into the recirculation region and the supply of hot combustion radicals

out into the main flow occurs through the detached shear layer. The shear layer growth and mass exchange depend on velocity ratio, density ratio, convective Mach numbers, heat release in combusting flow and pressure gradient. Within the shear layer scalar distributions vary widely and can have any value at a given instance from zero to one<sup>2</sup>.

A substantial database of flame stability exists for premixed gases<sup>3,4,5</sup> from which stability limits for rich and lean flames have been obtained for a number of fuels. The stability limit has usually been cast in terms of the flameholding boundary on an equivalence ratio vs. a stability parameter plane. These stability parameters depend on the flow velocity, temperature, size and shape of the flameholder and have received various formulations in different studies, from empirical formulations to expressions that reflect global Damköhler numbers.

In the case of non-premixed gases the determination of stability limits is less straightforward, primarily due to the non-homogeneity of the parameters in the recirculation region behind the flameholder. It is difficult to estimate the spatial species concentration and temperature distribution in the recirculation regions of these flows due to the presence of large gradients and the complex, 3-D, flow structure. These difficulties are compounded by the uncertainty in the shape of the recirculation region, which is a function of the amount of heat release which, in turn, is dictated by the local mixing and combustion efficiencies.

Driscoll<sup>6</sup> performed an analysis intended to lead to the development of a correlation for non-premixed flame stability limits in supersonic flow based on the suggestion that the flame base is sustained in the shear layer and not in the bulk of recirculation region. Flame propagation speed along the stoichiometric contour in the shear layer is matched, in this analysis, by the velocity of the incoming gas. Hot products in the recirculation zone preheat the shear layer gases and increase the flame propagation speed. Flame blowout is governed, then, by the imbalance between flame propagation speed and gas velocity. Some additional parameters governing blowout appeared in the non-premixed flame correlation compared to the premixed flame correlation: fuel injection location relative to the recirculation region, fuel injection temperature, and stoichiometric fuel mixture fraction. A limitation of this correlation is that a global fuel equivalence ratio was used for obtaining the flame stability curve, which is different from the local equivalence ratio in the flameholding recirculation region.

Winterfeld<sup>7</sup> performed flame blowout experiments in supersonic flow using a contoured cylindrical flameholder and a cone-cylinder flameholder. Hydrogen was injected into the recirculation region formed behind the flameholder at different angles relative to the airflow. The flame blowout curve was sensitive to the fuel injection angle. Hence the fuel injection location relative to the flameholding recirculation region is an important parameter in determining flame stability limits.

Ortwerth et al.<sup>1</sup> modified Ozawa's stability parameter for premixed gases<sup>3</sup> by including locally measured parameters in the recirculation region with limited success. The new parameter managed to describe a stability boundary for low equivalence ratios for hydrogen combustion but failed at injected equivalence ratios in excess of 0.1.

Sampling or optically-based methods used as a means of mapping the fuel distribution in non-premixed supersonic flows have been applied to a range of flowfields<sup>8,9,10</sup> and have shown that high local concentrations can persist for a long distance due to the characteristics of mixing layers growth and the role of large scale roll-

up layers. Similar mechanisms are also responsible for the mass transfer between a recirculation region and the flow that surrounds it, although a more complex situation arises due to the complicated streamlines geometry and the possible fuel injection or entrainment in this region.

The effect of various parameters on non-premixed flame stabilization in supersonic flow can be better understood by species composition measurements in the flameholding recirculation region. A few such measurements have been made for non-reacting flow experiments. Hsu et al.<sup>11</sup> used Raman scattering to make fuel distribution measurements inside a cavity in non-reacting supersonic flow. Ethylene was injected at a low angle upstream of the cavity. The effect of fuel injection pressure, cavity size, and imposed back-pressure on fuel transport in the cavity was studied. Following Hsu's experiments, Gruber et al.<sup>12</sup> made PLIF measurements in the cavity to examine the effect of fuel injection location on the cavity flameholder performance in supersonic flow for non-reacting flow and combustion experiments. Uchiumi et al.<sup>13</sup> followed up on the investigation by Niioka et al.<sup>14</sup> and conducted experiments to improve the flameholding performance of a strut divided into two parts in supersonic flow. Non-reacting flow measurements of local equivalence ratio along the distance between the strut parts were used to modify the strut configuration and improve its flameholding performance. Morrison et al.<sup>15</sup> performed flameholding experiments for a rearward step under ramjet conditions. The local equivalence ratio and mixing efficiency in the recirculation region behind the step were estimated by assuming premixed conditions in the region.

Numerical simulations of fuel mass fraction in the recirculation region for various flameholding geometries have also been performed. Kim et al.<sup>16</sup> investigated the flow oscillation over a cavity with fuel injected upstream and downstream of the cavity. The former produced significantly lower oscillations because it led to a more stable shear layer over the cavity. For downstream injection, fuel mass fraction contours showed that large vortices occurred that pulled the fuel upstream into the cavity. Gousskov et al.<sup>17</sup> investigated ignition and flameholding behind the base face of a strut in a supersonic combustion chamber. Both axisymmetric and 2D configurations were studied with hydrogen injected parallel to the airflow and into the recirculation region formed at the strut base. High water mass fraction distributions were found in the recirculation region for configurations in which the flame extended out from behind the strut into the main airflow. Glawe et al.<sup>18</sup> performed numerical simulations for helium injected at the base of a strut in supersonic flow. CFD contours showed a high helium mole fraction distribution in the recirculation region formed at the base of the strut.

There is a limited amount of experimental data regarding the composition of recirculation region in supersonic flow. The present study provides measurements under these conditions investigating non-premixed conditions in the recirculation region formed behind a rearward step in supersonic flow to expand current understanding of the flameholding mechanism in a scramjet engine combustor. A rearward-facing step was selected as the flameholder for its simple geometry. Non-reacting flow tests were performed, where the airflow parameters, i.e., Mach number, stagnation pressure and stagnation temperature were held constant and the fuel related parameters such as fuel type and injection pressure were varied. Local fuel mole fraction distribution in the recirculation region was measured in 2D plane using planar laser-induced fluorescence (PLIF) and point wise measurements were made using mass spectrometry (MS).

## Experimental setup

### Facility

The supersonic wind tunnel used in the experiments provides direct connect tests with a variable combustion chamber entrance Mach number of 1.6 - 3.6 and stagnation temperatures corresponding to Mach 4.8 flight enthalpy. The wind tunnel is a continuously operating facility using a vitiated heater based on hydrogen combustion with oxygen replenishment, electronically controlled by a fuzzy logic controller<sup>19</sup> to maintain a constant 0.21 oxygen mole fraction at all conditions and to maintain at the heater exit the constant stagnation temperature profile required for the experiment. A bellmouth with four-side contraction leads to the supersonic nozzle with compression on two sides and interchangeable nozzles that cover the range of Mach 1.6 - 3.6. All the experiments discussed here were performed with combustion chamber entrance Mach 1.6,  $P_{0\text{air}} = 4.8$  atm and ambient temperature air,  $T_{0\text{air}} = 300$  K. A constant area isolator is placed between the nozzle and the combustor section to reduce upstream interactions caused by pressure rise due to combustion in the test section. Optical access is available to the isolator and the test section. The isolator cross-section is  $2.5 \times 2.5$  cm<sup>2</sup> upstream of a rectangular, rearward facing step having step height  $H = 1.25$  cm and follows with a rectangular cross-section area test section  $26H$  in length. The test section is asymmetric with the step on one side and a flat wall on the other side. Fuel was injected transverse to the airflow and into the recirculation region at the base of the step as shown in Figure 1. Five 0.5-mm dia. holes equally spaced on each side of the test section wall were used. Helium and argon were injected as the simulated fuel.

### Mass spectrometry (MS)

The physical location of mass sampling ports in the recirculation region behind the step is shown in Figure 1. The coordinate system is also shown in the figure. These ports are 0.6 mm inner diameter steel tubes that end at the test section window wall and do not physically intrude into the recirculation region ( $z = 0$ ). In separate tests, other tubes are inserted from the window wall to investigate the three-dimensionality of species distribution in the recirculation region. In this case three stainless steel tubes are placed at  $x/H = 2.2$ ,  $y/H = 0.4$  and penetrate into the test section to sample species at three different depths, equally spaced in the inflow  $z$ -direction from  $z/W = 0.33$  to 1.0. Here  $W = 1.25$  cm is the test section half-width. Only inflow sampling results are described in this paper. The species were analyzed by Stanford Research Systems RGA-300 mass spectrometer. The mass sampling hardware and data analysis are described in more detail in ref. 20.

### Planar laser induced fluorescence (PLIF)

#### *Hardware*

Since mass spectrometry was limited to point-wise measurements in the flow, it was complemented by acetone Planar Laser Induced Fluorescence (PLIF) to obtain fuel distribution in a 2D plane in the recirculation region for non-reacting flow. The plane of

measurement was along the test section centerline at  $z/W = 1.0$ . A schematic diagram of the PLIF setup is shown in Figure 2. The test section used in PLIF measurements had step on only one side, unlike on both sides for the test section used in mass spectrometer measurements. However, since the airflow arriving at the step base is supersonic, the flow field in the recirculation region is the same for both test sections. The test section side wall window was made of glass for laser sheet delivery in the recirculation region. The test section front windows next to the step were also made of glass to provide visual access of the measurement plane via a camera. Before being injected in the test section, the fuel was seeded with acetone vapor by bubbling it into a chamber partially filled with liquid acetone at room temperature (295 K).

A pulsed Nd:YAG Spectra-Physics laser was used for LIF excitation of acetone. The laser pulsed at a frequency of 10 Hz and the fourth harmonic at 266 nm was used for acetone PLIF. At 266 nm wavelength, the laser pulse has 70 mJ energy and a pulse width of 4-5 ns. The beam diameter coming out of the laser was 7 mm that was converted into a sheet of light 40 mm wide and less than 0.5 mm thick at the step.

For image acquisition of acetone fluorescence in the visible spectrum, a Cooke Corporation intensified CCD camera and its associated software was used. The camera has a resolution of 1280 x 1024 pixels, 12-bit dynamic range and shutter speed down to 3 ns. The images were captured with an exposure time of 190 ms and a gain of 65%, with 100% representing the maximum gain achievable. A 2 x 2 binning was performed on the image in horizontal and vertical direction, that is, the average intensity of a square comprising 4 pixels was represented as the value for one pixel that replaced the 4 pixels.

### *Image Acquisition and Processing*

For each image acquisition, a total of 20 images were captured to get a time-averaged image over 1.2 s. Acetone condensation on the glass window due to low static temperature of main airflow was minimized by heating the glass window above the boiling temperature for acetone. The background image was subtracted from the experiment image. The laser sheet profile image was used to correct the experiment image for spatial non-uniformity in laser intensity using the following formula.

$$I_{corrected}(m, n) = I_{uncorrected}(m, n) * \frac{\max_{imum}[I_{laser}(m, p)]}{I_{laser}(m, p)}$$

where I: pixel intensity  
m, n: arbitrary row and column location of a pixel in the image  
p: a fixed column in the laser sheet image

The temperature distribution in the recirculation region is fairly uniform for non-reacting flows. Further, the acetone LIF signal does not vary with temperature for low temperature range of 200-300 K<sup>21,22</sup>. Hence the LIF signal intensity variation in the corrected image is independent of temperature and varies only with the concentration of acetone. The acetone LIF signal at the fuel injection location, where fuel mole fraction is 100 %, is taken as the reference point for other pixels in the image. The fuel mole

fraction at a given pixel is then determined by the ratio of LIF intensity at that pixel to the LIF intensity at the reference point.

For each experimental condition, image averaging from 3 repeatability experiments is used to remove variations from test to test. The fuel mole fraction distribution image, which does not depend on the laser intensity variation, is used to determine the average PLIF image for repeatability tests. Convolution filtering is applied on the averaged PLIF image and the fuel mole fraction distribution is obtained from the filtered image.

## Results

### Mass spectrometry (MS)

Non-reacting flow experiments were performed with helium and argon as the simulated fuels<sup>20</sup>. Mass sampling of the recirculation region species was done in the inflow  $z$ -direction with helium injected at the base of the step in  $P_{0\text{air}} = 4.8$  atm airflow. Helium was injected at two pressures, a moderate stagnation pressure  $P_{0\text{He}} = 5.4$  atm and a high stagnation pressure  $P_{0\text{He}} = 12.0$  atm. Each experiment was performed 3 times for repeatability. The inflow distribution of helium mole fraction ( $X_{\text{He}}$ ) in the recirculation region for the two helium stagnation pressures is shown in Figure 3 (a). The standard deviation bars are shown along with the average mole fractions for the repeated experiments. It is observed that increasing  $P_{0\text{He}}$  substantially results in a corresponding increase in  $X_{\text{He}}$  in the recirculation region. At both pressures, the inflow  $X_{\text{He}}$  are much higher than the wall measured  $X_{\text{He}}$ , specifically, up to 4-5 times.

Argon was injected at the base of the step for identical airflow and fuel injection conditions as in the case of helium injection. The inflow distribution of argon mole fraction ( $X_{\text{Ar}}$ ) in the recirculation region for the two argon stagnation pressures is shown in Figure 3 (b). The  $X_{\text{Ar}}$  distribution pattern is similar to that for helium injection, especially for low injection pressure. Away from the walls, the fuel distribution is uniform for low  $P_{0\text{Ar}}$  while non-uniformity is observed at high  $P_{0\text{Ar}}$ . The inflow  $X_{\text{Ar}}$  measurements are up to 2-3 times higher than the wall measured  $X_{\text{Ar}}$ .

### Planar laser induced fluorescence (PLIF)

PLIF imaging of the recirculation region fuel distribution in the centerline plane ( $z/W = 1.0$ ) was performed for identical airflow and fuel injection conditions as the mass sampling experiments. Each experiment was performed 3 times for repeatability. The results for helium injection are shown in Figures 4 and 5 for  $P_{0\text{He}} = 5.4$  atm and 12.0 atm respectively. The PLIF image for  $P_{0\text{He}} = 5.4$  atm is shown in Figure 4 (a) and the fuel mole fraction distribution is shown in Figure 4 (b). The expansion of airflow at the step pushed the shear layer towards the test section wall. The fuel injection holes are inclined relative to the step base. This is clearly visible in the figures as the fuel jet impinged on the step base and formed a plume above it. This fuel injection configuration helped the fuel remain and mix within the recirculation region. The PLIF image for  $P_{0\text{He}} = 12.0$  atm is shown in Figure 5 (a) and the fuel mole fraction distribution is shown in Figure 5 (b). In agreement with the mass spectrometer measurements, the fuel remained in the

recirculation region even as the injection pressure was increased. The fuel mole fraction distribution shows more non uniformity for higher injection pressure.

The global fuel mole fraction ( $X_{He}$ ), based on the total moles of fuel injected to the total moles of air flowing through the test section, was 1.13 % and 2.46 % for  $P_{0He} = 5.4$  atm and 12.0 atm respectively. The local  $X_{He}$  in the recirculation region and shear layer [Figure 4 (b) and 5 (b)] are an order of magnitude higher than the corresponding global  $X_{He}$  values. This is expected since only a fraction of the main airflow entered the recirculation region. The fuel lean condition suggested by global mole fraction is thus not a correct indicator of the much richer fuel composition existing in the recirculation region.

The results for argon injection are shown in Figures 6 and 7 for  $P_{0Ar} = 5.4$  atm and 12.0 atm respectively. The PLIF image for  $P_{0Ar} = 5.4$  atm is shown in Figure 6 (a) and the fuel mole fraction distribution is shown in Figure 6 (b). From Figures 4 and 6, it is seen that the fuel jet shear layer growth and mixing with ambient air in the recirculation region was higher for helium than argon. This is due to higher density ratio between air and helium than air and argon. The PLIF image for  $P_{0Ar} = 12.0$  atm is shown in Figure 7 (a) and the fuel mole fraction distribution is shown in Figure 7 (b). As in the case of helium injection, the fuel remained within the recirculation region for both injection pressures.

The global fuel mole fraction ( $X_{Ar}$ ), based on the total moles of fuel injected to the total moles of air flowing through the test section, was 0.36 % and 0.78 % for  $P_{0Ar} = 5.4$  atm and 12.0 atm respectively. As in helium injection, a much richer fuel composition existed in the recirculation region [Figure 6 (b) and 7 (b)] than suggested by global  $X_{Ar}$  values.

The fuel mole fraction measurements at  $x/H = 2.2$ ,  $y/H = 0.4$ ,  $z/W = 1.0$  obtained from PLIF and MS (Mass Spectrometry) are compared in Table 1 for various experimental conditions. The fuel mole fractions obtained from unfiltered image are reported for PLIF. Along with the average fuel mole fraction from 3 repeatability tests, the standard deviation is also indicated in brackets. The maximum standard deviation in fuel mole fraction is 2.4 % of the average for MS and 12.2 % for PLIF measurements. Hence data obtained from MS has less scatter than PLIF data. With PLIF data as the base, the difference between average fuel mole fractions obtained from PLIF and MS is 11.4 - 22.9 %. For higher injection pressure of both helium and argon, the PLIF and MS data range overlap with each other. The observed difference between PLIF and MS measurements can be due to several factors. The variation in laser sheet profile from test to test has not been taken into consideration. Since mass spectrometry is an intrusive technique, disturbances to the flow field due to the presence of sampling ports and gas suction cannot be eliminated completely. The PLIF data is reported at 1 pixel, while MS data is acquired for 7 pixels diameter circular cross section of the sampling tube. The data from the two experimental techniques are compared only at a single point in the flow field. A slight misalignment of the measurement point between the two techniques can cause difference in data due to gradients in the flow field. Hence data from the two techniques could be compared at more measurement points.

## Conclusions

Planar Laser Induced Fluorescence (PLIF) and mass spectrometry (MS) were used to determine the fuel mole fraction distribution in the recirculation region and shear layer formed behind a rectangular step in non-reacting supersonic flow. The results indicated the following:

- The local fuel composition in the recirculation region was an order of magnitude higher than the suggested global fuel mole fraction since only a small part of the main airflow entered the recirculation region.
- Fuel injected at the step base remained in the recirculation region and shear layer for all experimental conditions investigated in the study.
- Fuel distribution in the recirculation region was more non-uniform for higher fuel injection pressure.
- The injected fuel jet mixed faster with ambient air in the recirculation region for helium than argon. The shear layer growth rate for air and helium is faster than air and argon due to higher density ratio.
- The average fuel mole fractions obtained from MS and PLIF differ by 11.4 - 22.9 %; the data range from the two techniques overlap for higher helium and argon injection pressures. Fuel mole fraction measurements from MS show less scatter than those obtained from PLIF.

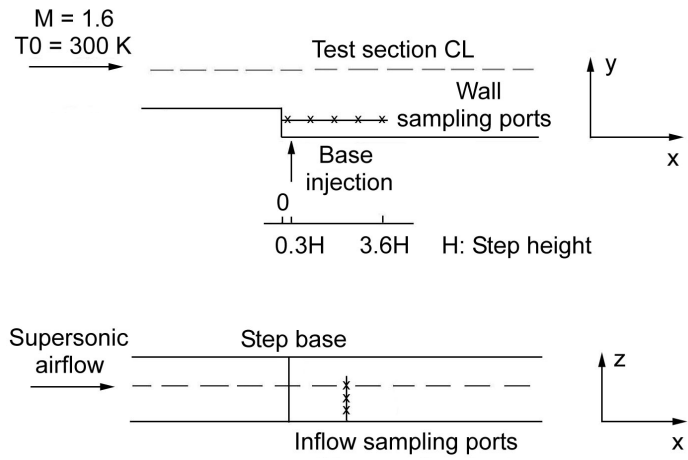


Figure 1. Schematic diagram of the test section showing fuel injection and mass sampling locations.

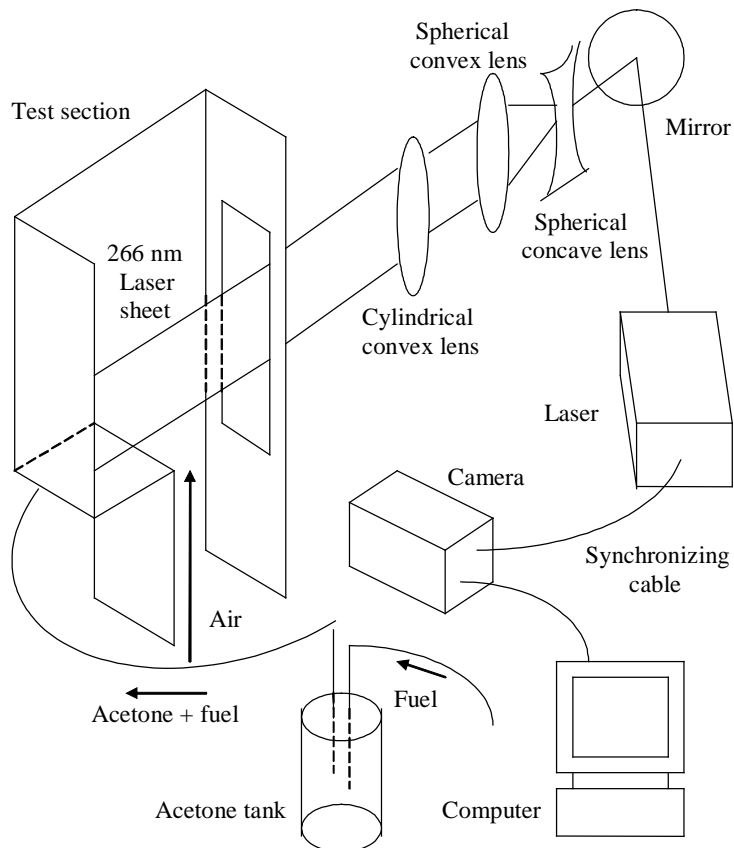
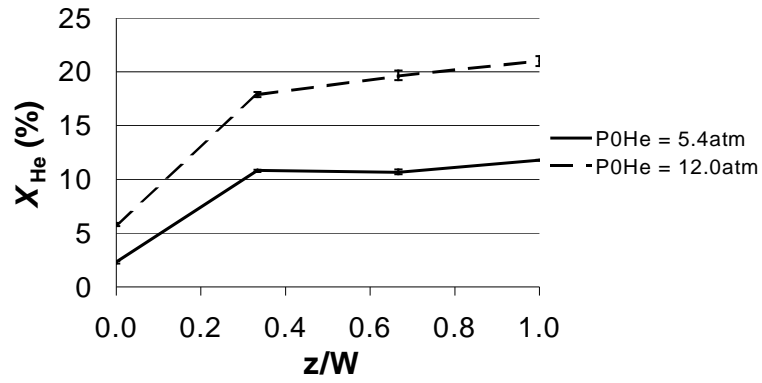
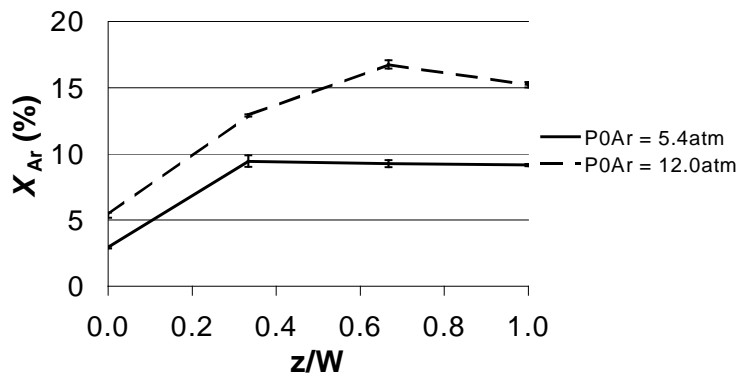


Figure 2. Schematic diagram of Planar Laser-Induced Fluorescence (PLIF) setup.



(a)



(b)

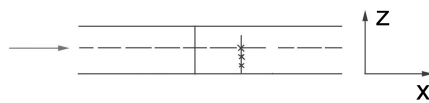


Figure 3. Inflow mole fraction measurements from mass spectrometer for (a) helium (b) argon injection.

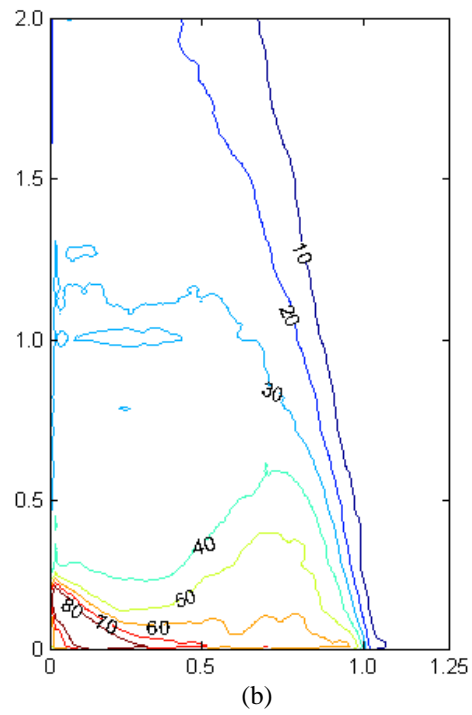
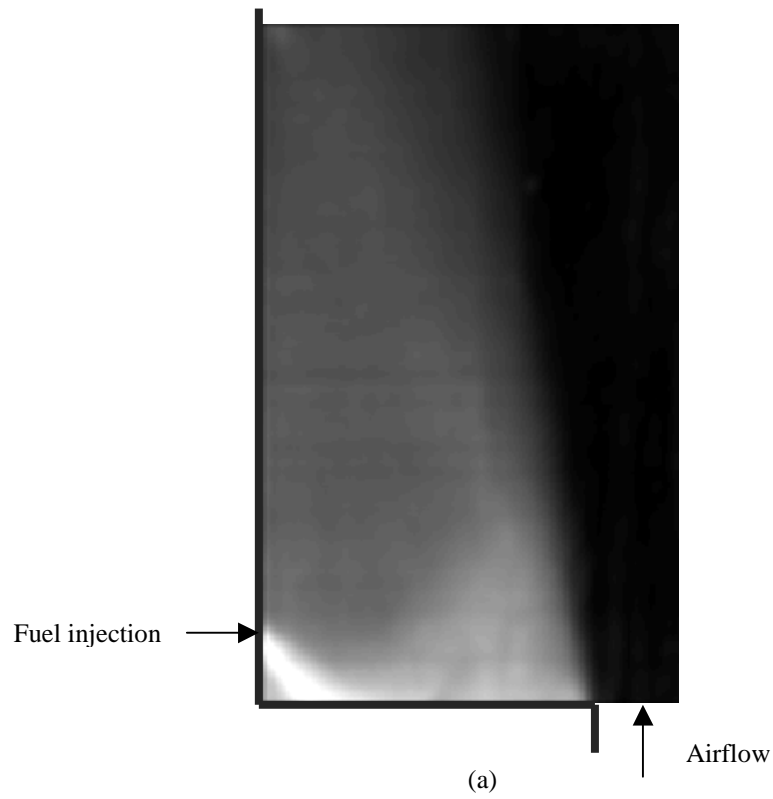


Figure 4. PLIF measurements for  $P_{0\text{He}} = 5.4 \text{ atm}$  (a) image (b) mole fraction distribution.

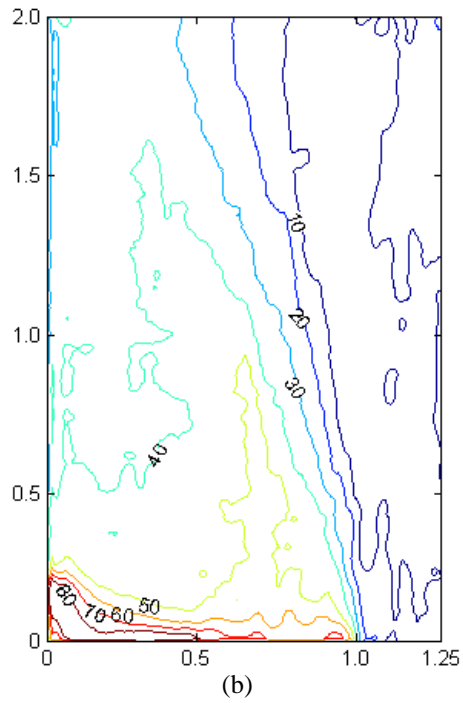
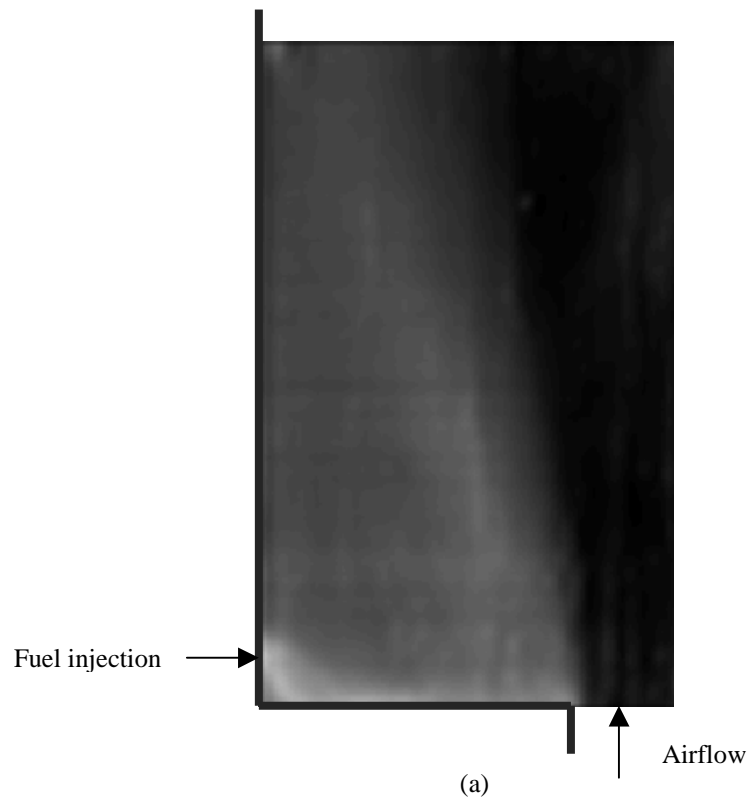


Figure 5. PLIF measurements for  $P_{0\text{He}} = 12.0$  atm (a) image (b) mole fraction distribution.

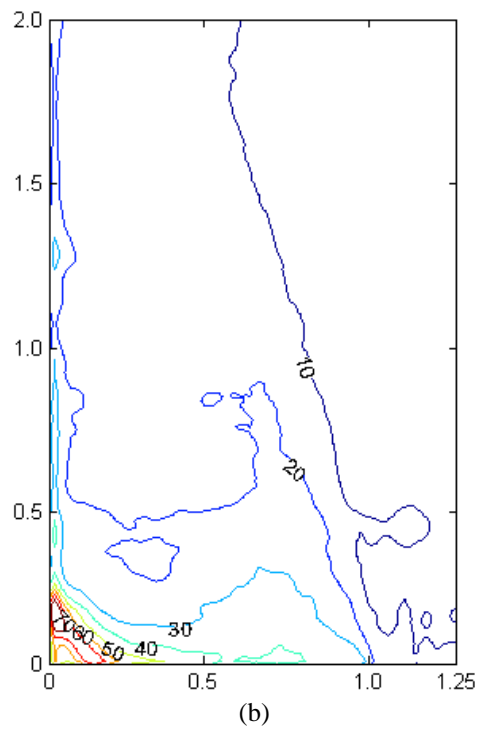
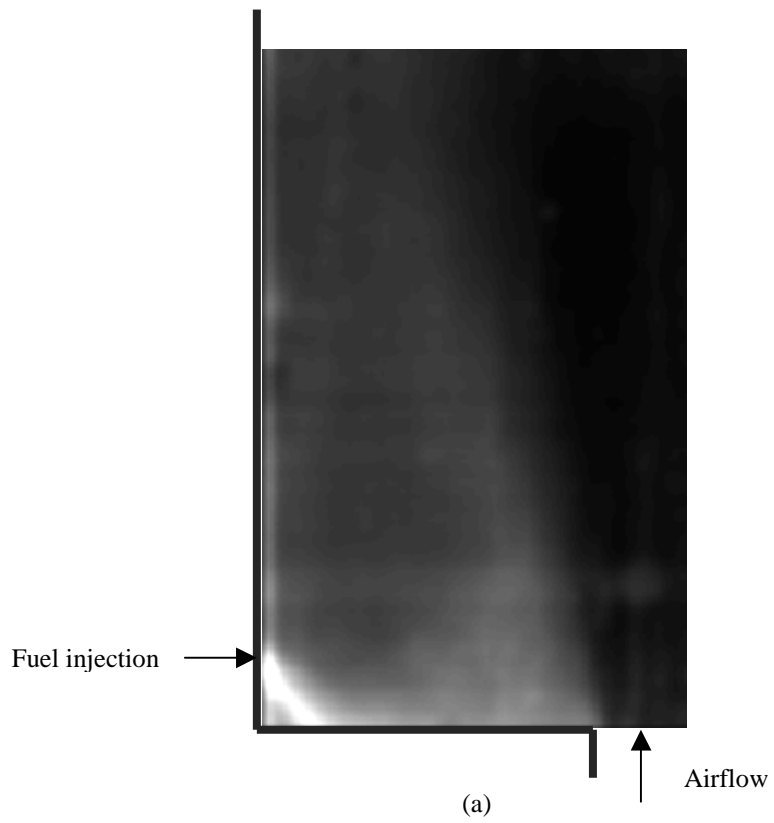


Figure 6. PLIF measurements for  $P_{0Ar} = 5.4$  atm (a) image (b) mole fraction distribution.

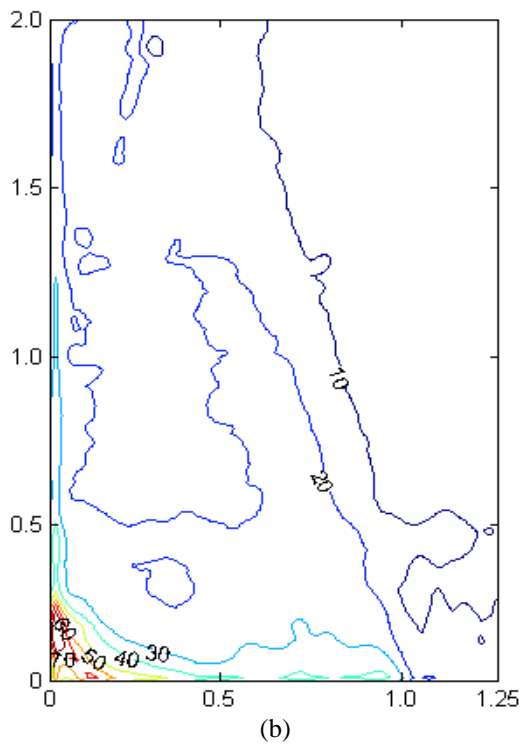
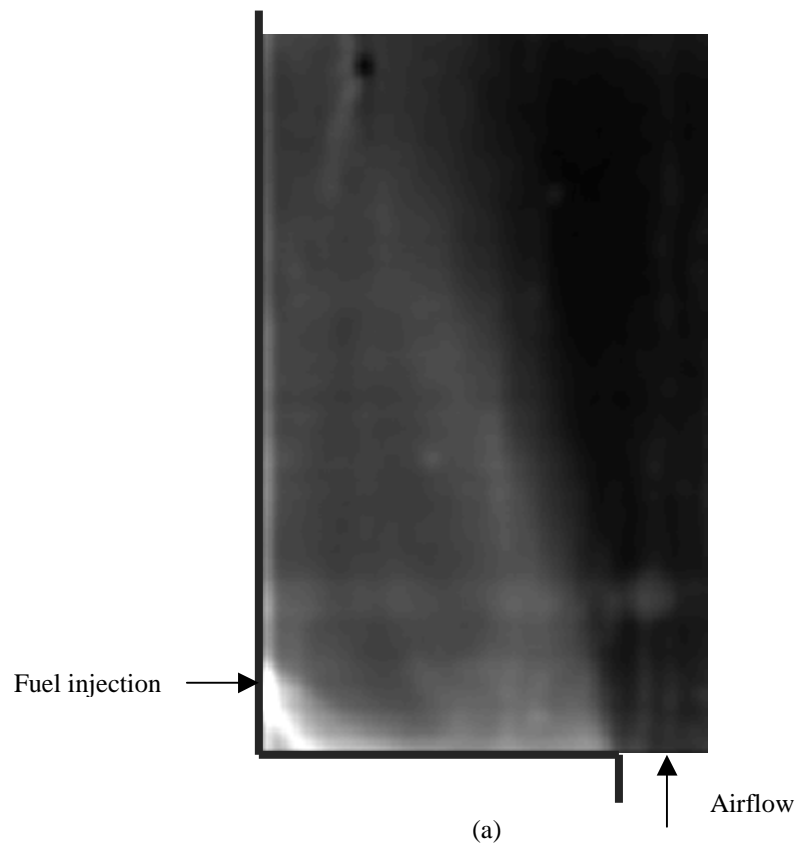


Figure 7. PLIF measurements for  $P_{0Ar} = 12.0$  atm (a) image (b) mole fraction distribution.

Table 1. Comparison of PLIF and MS fuel mole fraction measurements.

Experimental condition	Global $X_{\text{fuel}}$ (%)	PLIF $X_{\text{fuel}}$ (%)	MS $X_{\text{fuel}}$ (%)	% difference
$P_{0\text{He}} = 5.4 \text{ atm}$	1.13	15.3 (1.8)	11.8 (0.02)	22.9
$P_{0\text{He}} = 12.0 \text{ atm}$	2.46	23.7 (2.7)	21.0 (0.5)	11.4
$P_{0\text{Ar}} = 5.4 \text{ atm}$	0.36	11.4 (1.4)	9.2 (0.1)	19.3
$P_{0\text{Ar}} = 12.0 \text{ atm}$	0.78	13.4 (1.6)	15.2 (0.2)	13.4

## References

- <sup>1</sup> Ortwerth P. J., Mathur A. B., Segal C., Mullagilli S., "Combustion Stability Limits of Hydrogen in a Non-Premixed, Supersonic Flow", *Proceedings of ISABE 99*, Paper 99-143, 1999.
- <sup>2</sup> Dimotakis P. E., "Turbulent free shear layer mixing and combustion", High-speed Flight Propulsion Systems, Murthy S. N. B. and Curran E. T. - editors, *Progress in Aeronautics and Astronautics*, Vol. 137, pp. 265-340, 1991.
- <sup>3</sup> Ozawa R. I., "Survey of Basic Data on Flame Stabilization and Propagation for High Speed Combustion Systems", The Marquart Co., TR AFAPL-TR-70-81, Jan. 1971.
- <sup>4</sup> Huellmantel L. W., Ziemer R. W., Cambel A. B., "Stabilization of Premixed Propane-Air Flames in Recessed Ducts", *Journal of Jet Propulsion*, pp. 31-43, Jan. 1957.
- <sup>5</sup> Ogorodnikov D. A., Vinogradov V. A., Shikhman Y. M., Strokin V. N., "Russian Research on Experimental Hydrogen-Fueled Dual-Mode Scramjet: Conception and Preflight Tests", *Journal of Propulsion and Power*, Vol. 17, No. 5, pp. 1041-1048, 2001.
- <sup>6</sup> Driscoll J. F., Rasmussen C. C., "Correlation and analysis of blowout limits of flames in high-speed airflows", *Journal of Propulsion and Power*, Vol. 21, No. 6, pp. 1035-1044, 2005.
- <sup>7</sup> Winterfeld G., "Stabilization of hydrogen-air flames in supersonic flow", *Modern research topics in aerospace propulsion*, pp. 37-47, 1991.
- <sup>8</sup> Rogers R. C., "A Study of the Mixing of Hydrogen Injected Normal to a Supersonic Airstream", *NASA Technical Note*, TN D-6114, 1971.
- <sup>9</sup> Cox S. K., Fuller R. P., Schetz J. A., Walters R. W., "Vortical Interactions Generated by an Injector Array to Enhance Mixing in Supersonic Flow", *32<sup>nd</sup> Aerospace Sciences Meeting and Exhibit*, AIAA 94-0708, 1994.
- <sup>10</sup> VanLerberghe W. M., Santiago J. C., Dutton J. C., Lucht R. P., "Mixing of a Sonic Transverse Jet Injected into a Supersonic Flow", *AIAA Journal*, Vol. 38, No. 3, pp. 470-479, March 2000.
- <sup>11</sup> Hsu K.Y., Carter C. D., Crafton J., Gruber M. R., Donbar J. M., Mathur T., Schommer D., Terry W., "Fuel distribution about a cavity flameholder in supersonic flow", *AIAA Paper*, AIAA-2000-3585, 2000.
- <sup>12</sup> Gruber M. R., Donbar J. M., Carter C. D., Hsu K. Y., "Mixing and combustion studies using cavity based flameholders in a supersonic flow", *Journal of Propulsion and Power*, Vol. 20 (5), pp. 769-778, 2004.
- <sup>13</sup> Uchiumi M., Kobayashi H., Hasegawa S., Niioka T., "Experiments on the flameholding mechanism of a newly devised strut in supersonic airflow", *IUTAM Symposium on Combustion in Supersonic Flows*, Champion M. and Deshaies B. - editors, pp. 135-144, 1997.
- <sup>14</sup> Niioka T., Terada K., Kobayashi H., Hasegawa S., "Flame stabilization characteristics of strut divided into two parts in supersonic flow", *Journal of Propulsion and Power*, Vol. 11 (1), pp. 112-116, 1995.
- <sup>15</sup> Morrison C. Q., Campbell R. L., Edelman R. B., Jaul W. K., "Hydrocarbon fueled dual mode ramjet/scramjet concept evaluation", *Proceedings of the International Society for Air-breathing Engines*, ISABE-1997-7053, pp. 348-356, 1997.

- 
- <sup>16</sup>Kim C. K., Yu S. T., Zhang Z. C., “Cavity flow in scramjet engine by space-time conservation and solution element method”, *AIAA Journal*, Vol. 42 (5), pp. 912-919, 2004.
- <sup>17</sup>Gousskov O. V., Kopchenov V. I., “Investigation of ignition and flame stabilization behind the strut in supersonic flow”, 2002.
- <sup>18</sup>Glawe D. D., Donbar J. M., Nejad A. S., Sekar B., Chen T. H., Samimy M., Driscoll J. F., “Parallel fuel injection from the base of an extended strut into supersonic flow”, *AIAA Paper*, AIAA-1994-0711, 1994.
- <sup>19</sup>Owens M., Segal C., “Development of a Hybrid-Fuzzy Air Temperature Controller for a Supersonic Combustion Test Facility”, *Experiments in Fluids*, Vol. 31, no. 1, pp. 26-33, 2001.
- <sup>20</sup>Thakur A., Segal C., “Flameholding Analyses in supersonic Flow”, *AIAA Paper*, AIAA 2004-3831, 2004.
- <sup>21</sup>Lozano A., Yip B., Hanson R. K., “Acetone: a tracer for concentration measurements in gaseous flows by planar laser-induced fluorescence”, *Experiments in Fluids*, Vol. 13, pp. 369-376, 1992.
- <sup>22</sup>Bryant R. A., Donbar J. M., Driscoll J. F., “Acetone LIF for flow visualization at temperatures below 300K”, *AIAA Paper*, AIAA-1997-0156, 1997.